

# Onset of convection over a transient base-state in anisotropic and layered porous media

SAIKIRAN RAPAKA<sup>1,†</sup>, RAJESH J. PAWAR<sup>3</sup>,  
PHILIP H. STAUFFER<sup>3</sup>, DONGXIAO ZHANG<sup>4</sup>  
AND SHIYI CHEN<sup>1,2</sup>

<sup>1</sup>Department of Mechanical Engineering, Johns Hopkins University, Baltimore, MD 21218, USA

<sup>2</sup>SKLTCS & CAPT, College of Engineering, Peking University, Beijing 100871, P.R. China

<sup>3</sup>EES-6, Los Alamos National Laboratory, Los Alamos, NM 87544, USA

<sup>4</sup>Department of Civil and Environmental Engineering, University of Southern California,  
Los Angeles, CA 90089, USA

(Received 9 March 2009; revised 3 August 2009; accepted 4 August 2009; first published online  
16 November 2009)

The topic of density-driven convection in porous media has been the focus of many recent studies due to its relevance as a long-term trapping mechanism during geological sequestration of carbon dioxide. Most of these studies have addressed the problem in homogeneous and anisotropic permeability fields using linear-stability analysis, and relatively little attention has been paid to the analysis for heterogeneous systems. Previous investigators have reduced the governing equations to an initial-value problem and have analysed it either with a quasi-steady-state approximation model or using numerical integration with arbitrary initial perturbations. Recently, Rapaka *et al.* (*J. Fluid Mech.*, vol. 609, 2008, pp. 285–303) used the idea of non-modal stability analysis to compute the maximum amplification of perturbations in this system, optimized over the entire space of initial perturbations. This technique is a mathematically rigorous extension of the traditional normal-mode analysis to non-normal and time-dependent problems. In this work, we extend this analysis to the important cases of anisotropic and layered porous media with a permeability variation in the vertical direction. The governing equations are linearized and reduced to a set of coupled ordinary differential equations of the initial-value type using the Galerkin technique. Non-modal stability analysis is used to compute the maximum growth of perturbations along with the optimal wavenumber leading to this growth. We show that unlike the solution of the initial-value problem, results obtained using non-modal analysis are insensitive to the choice of bottom boundary condition. For the anisotropic problem, the dependence of critical time and wavenumber on the anisotropy ratio was found to be in good agreement with theoretical scalings proposed by Ennis-King *et al.* (*Phys. Fluids*, vol. 17, 2005, paper no. 084107). For heterogeneous systems, we show that uncertainty in the permeability field at low wavenumbers can influence the growth of perturbations. We use a Monte Carlo approach to compute the mean and standard deviation of the critical time for a sample permeability field. The results from theory are also compared with finite-volume simulations of the governing equations using fully heterogeneous porous media with strong layering. We show that the results from non-modal stability analysis match extremely well with those obtained from the simulations as long as the assumption of strong layering remains valid.

† Email address for correspondence: saikiran@jhu.edu

**Key words:** absolute/convective, instability, porous media

---

## 1. Introduction

Geological sequestration of carbon dioxide ( $\text{CO}_2$ ) into saline aquifers is considered to be one of the most promising short-term solutions to mitigating greenhouse gas emissions (IPCC 2005). The process involves capturing and pumping  $\text{CO}_2$  produced at large industries and power plants into aquifers at a depth more than 800 m below the surface of earth. Under the conditions present in these aquifers,  $\text{CO}_2$  exists in a supercritical state with a density lower than that of the surrounding brine. The injected  $\text{CO}_2$  rises upwards due to buoyancy and settles under the low-permeability caprock (Hitchon 1996). Over a period of many decades following injection, the  $\text{CO}_2$  slowly dissolves into the underlying brine. This solution of brine saturated with  $\text{CO}_2$  has a density slightly higher (by about 1%) than that of pure brine (Garcia 2001), resulting in a gravitational instability. Under suitable conditions, this instability manifests itself in the form of fingers of  $\text{CO}_2$ -rich brine penetrating downwards. This convective mechanism is expected to greatly enhance the rate of dissolution of  $\text{CO}_2$  resulting in faster localization of the injected  $\text{CO}_2$ .

Due to the importance of density-driven convection process, there has been renewed interest in studying the onset of convection along with the associated length and time scales. Historically, the earliest work on convection in porous media was by Horton & Rogers (1945) and Lapwood (1948), who studied the onset of cellular convection over a linear, steady-state temperature profile in isotropic porous media using linear-stability theory. These results were found to be in good agreement with experiments and numerical simulations (Cheng 1978). A large body of work has focused on understanding this cellular mode of convection (see for instance Beck 1972), and a good review of the existing work is provided by Nield & Bejan (2006). The analysis was extended to the case of anisotropic media by Castinel & Combarous (1977), Epherre (1977) and Kvernfold & Tyvand (1979) who used linear-stability theory to derive the critical Rayleigh number for anisotropic media. Wooding (1978) presented criteria for the onset of convection in media in which the permeability varies in the vertical direction. Nield (1997) introduced the idea of an effective Rayleigh number using the square of the harmonic mean of square roots of permeability. The case in which one of the principal axes of permeability is not aligned with the direction of gravity was analysed by Tyvand & Storesletten (1991). A nonlinear-stability analysis for the anisotropic case was performed by Nilsen & Storesletten (1990).

The onset of convection in layered media was studied by McKibbin & O'Sullivan (1980) who analysed two- and three-layered media with varying contrasts of permeability. McKibbin & Tyvand (1982) showed that the large-scale convection in multi-layered porous media converges to the homogeneous anisotropic model as the number of layers increases. Systems with vertically varying permeability were considered by Nield (1994) and Leong & Lai (2001), and Braester & Vadasz (1993) studied the effects of a weak heterogeneity using a perturbative approach. Simmons, Fenstermaker & Sharp (2001) and Prasad & Simmons (2003) studied the Elder problem (Elder 1967) in heterogeneous media and concluded that the traditional Rayleigh-number-based criteria is not adequate for heterogeneous systems. Subsequently, Nield & Simmons (2007) emphasized the need to identify between strong and weak heterogeneity and argued that the idea of an effective Rayleigh number is useful for the case of weak heterogeneity.

The problem considered in this work differs from the Horton–Rogers problem due to the time dependence of the base-state. We consider a quiescent porous medium with initially no dissolved  $\text{CO}_2$  in contact with an infinite source of  $\text{CO}_2$  at the top of the domain. The analogous case for heat transfer would be a system which is suddenly cooled at the top. Mathematically, we specify that the brine lying at the interface with supercritical  $\text{CO}_2$  is saturated with  $\text{CO}_2$ . Much work has been done on describing the stability of time-dependent systems. One early approach is the so-called quasi-steady-state analysis, which involves ‘freezing’ the base-state at some initial time  $t_0$  and studying the dynamics of the perturbations on the nonlinear base-state (Lick 1965; Currie 1967). In this approach the main assumption is that the perturbations are evolving much faster than the base-state, and the time dependence of the base-state only enters through the parameter  $t_0$ . Another approach is to use a suitably selected eigenfunction decomposition to convert the partial differential equations (PDEs) into a set of coupled ordinary differential equations (ODEs) of the initial-value kind (Foster 1965) for the coefficients of the expansion. One problem with this approach is that the initial conditions required to solve the ODEs are not known. Foster (1965) studied the dynamics of this system for many different initial conditions and found that a ‘white-noise’ initial condition in which all the coefficients are set to unity gives the fastest growth. Tan & Homsy (1986) compared the quasi-steady-state analysis approach to the initial-value approach and found that except for a brief period when the base-state is changing rapidly, the two approaches give comparable results. Jhaveri & Homsy (1982) used a stochastic formulation in which the amplitude of the random forcing was computed using statistical thermodynamics. An approach complementary to linear stability is the energy technique (Joseph 1976; Straughan 2004) in which one studies the dynamics of a suitable defined energy functional.

Following Foster (1965), many investigators have recently used the initial-value approach to analyse the carbon sequestration problem (Ennis-King, Preston & Paterson 2005; Hassanzadeh, Pooladi-Darvish & Keith 2006; Xu, Chen & Zhang 2006). Ennis-King *et al.* (2005) used linear-stability analysis and global-stability analysis to provide bounds for the length and time scales of convection in anisotropic porous media. They also used the single-term Galerkin solution to obtain analytical scalings for the dependence of critical time and wavenumbers on the anisotropy ratio. Xu *et al.* (2006) extended these results by considering the variation of both horizontal and vertical permeability. Hassanzadeh *et al.* (2006) used initial conditions with different spectra to study the influence of initial conditions on the growth of perturbations. In principle, we would like to use the optimal (fastest growing) perturbations to study the length and time scales of convection. Riaz *et al.* (2006) studied the problem for isotropic media using a co-ordinate transformation to a similarity variable. They have shown that the solution resolves to the dominant mode rapidly in this formulation, allowing them to study the dynamics of only the dominant mode. Kim & Choi (2007) used a relaxed energy stability approach to predict the critical length and time scales for a semi-infinite system and compared their results with those obtained by previous investigators.

Recently, Rapaka *et al.* (2008) used the idea of non-modal stability theory (Farrell & Ioannou 1996*a,b*; Trefethen & Embree 2005; Schmid 2007) to compute the maximum amplification obtained by perturbations, optimized over the entire space of initial conditions. They also obtained the physical structure of the optimal perturbation and showed an excellent match with three-dimensional direct numerical simulations of the governing equations. In this paper, we extend this work to account for the effects of anisotropy and horizontal layering of the medium. In §2, we describe the governing equations for the system and derive the ODEs for the linearized system. Section 3

provides a brief introduction to the idea of non-modal stability and the mechanism for the onset of convection. In §4 we present the results for anisotropic systems, and §5 presents stability results for layered porous media along with a comparison with finite-volume computations. Finally we present some concluding remarks in §6.

## 2. Governing equations

The basic equations governing flow and transport in porous media are Darcy's law for the momentum of the fluid, continuity equation enforcing conservation of mass and an advection–diffusion equation for the concentration of dissolved CO<sub>2</sub>:

$$\mu \mathbf{K}^{-1} \cdot \mathbf{v} = -\nabla P + \rho_f g \mathbf{e}_z, \quad (2.1)$$

$$\frac{\partial \rho_f}{\partial t} + \nabla \cdot (\rho_f \mathbf{v}) = 0, \quad (2.2)$$

$$\phi \frac{\partial C}{\partial t} + \nabla \cdot (\mathbf{v} C) = \phi D \nabla^2 C, \quad (2.3)$$

where  $\mu$  is the viscosity of the fluid;  $\mathbf{v} = (u, v, w)$  is the volumetric flux of fluid (Stauffer 2006);  $P$  is the pressure;  $\rho_f$  is the density of the brine–CO<sub>2</sub> mixture;  $g$  is the acceleration due to gravity;  $C$  is the concentration of dissolved CO<sub>2</sub>;  $\phi$  is the porosity; and  $D$  is the diffusion coefficient of CO<sub>2</sub> in brine. The volumetric flux  $\mathbf{v}$  includes the effects of local porosity of the rock. For convenience, we will henceforth refer to  $\mathbf{v}$  as the ‘velocity’ of the fluid. The tensor  $\mathbf{K}$  is the permeability tensor, which is taken to be of the following form in this paper:

$$\mathbf{K} = \begin{pmatrix} K_H & 0 & 0 \\ 0 & K_H & 0 \\ 0 & 0 & \gamma K_H \end{pmatrix}, \quad (2.4)$$

where  $K_H$  is the permeability in the horizontal directions and  $\gamma \leq 1.0$  is the constant anisotropy ratio. For cases in which we are interested in the effects of heterogeneity, we take  $\gamma = 1$  and  $K_H$  to be a function of the vertical direction,  $K_H = K_H(z)$ . Many reservoirs and aquifers are composed of layers with different permeabilities, and studying such systems is of great interest to petroleum exploration, modelling contaminant transport and understanding geothermal convection. Experimental studies on the equation of state of the brine–CO<sub>2</sub> system have shown that the density of the mixture is approximately linear in the concentration of dissolved CO<sub>2</sub> within the range of pressures and temperatures of interest (Garcia 2001):

$$\rho_f = \rho_0 (1 + \beta C), \quad (2.5)$$

where  $\beta = (1/\rho_0) \partial \rho_f / \partial C$ . Also, since the total change in density under saturated conditions is less than 1%, we work in the framework of Boussinesq approximation, replacing  $\rho_f$  by  $\rho_0$  everywhere, except in the buoyancy term.

In this paper, we are concerned with two separate, but closely related, problems: (i) the effect of anisotropy and (ii) the effect of vertical heterogeneity (layering) on the critical time and length scales characteristic of convection. While studying the effects of anisotropy,  $K_H$  is taken to be a constant value with no spatial dependence, whereas for the heterogeneous cases, we use  $\gamma = 1.0$  (i.e. locally isotropic) and  $K_H$  varies in the vertical direction. This vertical variation of permeability can be shown to lead to global anisotropy when the number of layers is large (for the convergence of a layered model to the anisotropic case, see McKibbin & Tyvand 1982).

2.1. Formulation for the anisotropy problem

Following Ennis-King *et al.* (2005), we non-dimensionalize the governing equations using

$$\begin{aligned} \hat{x} &= \frac{x\sqrt{\gamma}}{H}, & \hat{y} &= \frac{y\sqrt{\gamma}}{H}, & \hat{z} &= \frac{z}{H}, \\ \hat{u} &= \frac{uH\sqrt{\gamma}}{\phi D}, & \hat{v} &= \frac{vH\sqrt{\gamma}}{\phi D}, & \hat{w} &= \frac{wH}{\phi D}, \\ \hat{C} &= \frac{C}{C_0}, & \hat{P} &= \frac{P\gamma K_H}{\mu\phi D}, & \hat{t} &= \frac{tD}{H^2}. \end{aligned}$$

In the following discussion, we omit the hats over the non-dimensional variables for simplicity. The resulting non-dimensional equations are

$$\mathbf{v} = -\nabla P + \gamma Ra C \mathbf{e}_z, \tag{2.6}$$

$$\nabla \cdot \mathbf{v} = 0, \tag{2.7}$$

$$\frac{\partial C}{\partial t} + \nabla \cdot (\mathbf{v}C) = \gamma \nabla_H^2 C + \frac{\partial^2 C}{\partial z^2}, \tag{2.8}$$

where  $Ra$  is the Rayleigh number, defined as

$$Ra = \frac{K_H \rho_0 \beta C_0 g H}{\mu \phi D}. \tag{2.9}$$

Eliminating pressure from the momentum equation, we get

$$\nabla^2 w = \gamma Ra \nabla_H^2 C, \tag{2.10}$$

where  $\nabla_H^2 = (\partial^2/\partial x^2) + (\partial^2/\partial y^2)$  is the Laplacian in the horizontal directions. The boundary conditions for the velocity and concentration fields are

$$w(z = 0) = 0, \quad w(z = 1) = 0, \tag{2.11}$$

$$C(z = 0) = 1, \quad \frac{\partial C}{\partial z}(z = 1) = 0. \tag{2.12}$$

2.2. Formulation for the heterogeneous problem

In this case, the permeability is locally isotropic (i.e.  $\gamma = 1.0$ ) and can be given by a single function  $K(z)$ . For convenience, we define the resistance function,  $R(z) = K(z)^{-1}$ . Non-dimensionalizing the equations as before, we get

$$R(z)\mathbf{v} = -\nabla P + Ra C \mathbf{e}_z, \tag{2.13}$$

$$\nabla \cdot \mathbf{v} = 0, \tag{2.14}$$

$$\frac{\partial C}{\partial t} + \nabla \cdot (\mathbf{v}C) = \nabla^2 C, \tag{2.15}$$

where the Rayleigh number is now defined as

$$Ra = \frac{K_0 \rho_0 \beta C_0 g H}{\mu \phi D}. \tag{2.16}$$

The global Rayleigh number depends on a permeability scale  $K_0$ , the choice of which is non-trivial (for a discussion, refer to Nield & Simmons 2007). In this work, we choose  $K_0$  to be the harmonic mean of the permeability. Taking the curl of the momentum equation twice, we obtain

$$\nabla(\nabla \cdot (R\mathbf{v})) - \nabla^2(R\mathbf{v}) = -\gamma Ra \nabla_H^2 C \mathbf{e}_z. \tag{2.17}$$

Using the incompressibility constraint, this equation can be simplified to

$$R\nabla^2 w + R'w' = Ra\nabla_H^2 C, \quad (2.18)$$

where the primes denote differentiation along the vertical direction.

### 3. Linear analysis: non-modal growth

For both the anisotropic and heterogeneous formulations, the vertical component of velocity is related to the concentration field through a linear operator  $\mathcal{L}$ . For simplicity, we will just refer to the velocity equation as

$$\mathcal{L}w = Ra\nabla_H^2 C,$$

where for the anisotropic problem the operator  $\mathcal{L}$  is

$$\mathcal{L} = \frac{1}{\gamma}\nabla^2,$$

and for the heterogeneous problem

$$\mathcal{L} = R\nabla^2 + R'\frac{d}{dz}.$$

We now formally separate the pressure and concentration of dissolved CO<sub>2</sub> into a base-state and superimposed perturbations of initial magnitude  $\epsilon$ :

$$C = C_{ref} + \epsilon\theta, \quad P = P_{ref} + \epsilon\Pi.$$

When these are substituted into the governing equations with terms  $O(\epsilon^2)$  being ignored and the equation analysed at different orders of  $\epsilon$ , we get at  $O(\epsilon^0)$

$$\frac{\partial C_{ref}}{\partial t} = \frac{\partial C_{ref}}{\partial z^2}, \quad (3.1)$$

$$C_{ref}(z = 0, t) = 1, \quad \frac{\partial C_{ref}}{\partial z}(z = 1, t) = 0, \quad C_{ref}(z, t = 0) = 0.$$

The vertical velocity equation, being linear, is unaffected,

$$\mathcal{L}w = Ra\nabla_H^2 \theta, \quad (3.2)$$

with the following boundary conditions:

$$w(z = 0) = 0, \quad w(z = 1) = 0.$$

Finally, the linearized dynamics of the perturbation are given by:

$$\frac{\partial \theta}{\partial t} + w\frac{dC_{ref}}{dz} = \nabla_H^2 \theta + \frac{\partial^2 \theta}{\partial z^2}, \quad (3.3)$$

$$\theta(z = 0, t) = 0, \quad \frac{\partial \theta}{\partial z}(z = 1, t) = 0.$$

We now take the vertical velocity and the concentration perturbation to be wave-like in the horizontal direction and expand them in terms of suitable eigenfunctions satisfying the boundary conditions in the vertical direction:

$$w = \sum_n \hat{w}_n e^{ik \cdot x} \sin(n\pi z), \quad (3.4)$$

$$\theta = \sum_n \hat{\theta}_n e^{ik \cdot x} \sin\left(\left(n - \frac{1}{2}\right)\pi z\right). \quad (3.5)$$

After substitution of these equations in the linearized governing equations and use of the Galerkin technique, the PDEs can be reduced to a set of coupled ODEs of the initial-value type for the coefficients  $\widehat{\theta}_n$ ,

$$\frac{d}{dt}\widehat{\theta}_n = \mathbf{G}_{nm}\widehat{\theta}_m, \tag{3.6}$$

where the matrix  $\mathbf{G}$  for the anisotropy problem is given by

$$\mathbf{G} = \mathbf{A}^{-1}[\mathbf{B} - \gamma Ra_h \mathbf{C} \mathbf{E}^{-1} \mathbf{D}], \tag{3.7}$$

$$A_{nm} = \frac{1}{2}\delta_{nm}, \tag{3.8}$$

$$B_{nm} = -\frac{1}{2} \left[ \gamma k^2 + \left(m - \frac{1}{2}\right)^2 \pi^2 \right] \delta_{nm}, \tag{3.9}$$

$$C_{nm} = -\frac{1}{2} \left[ \exp \left\{ - \left(m + n - \frac{1}{2}\right)^2 \pi^2 t \right\} - \exp \left\{ - \left(m - n + \frac{1}{2}\right)^2 \pi^2 t \right\} \right], \tag{3.10}$$

$$D_{nm} = (-1)^{n+m} \frac{s^2 n}{\pi \left(n + m - \frac{1}{2}\right) \left(n - m + \frac{1}{2}\right)}, \tag{3.11}$$

$$E_{nm} = -\frac{1}{2}(k^2 + m^2 \pi^2) \delta_{nm}, \tag{3.12}$$

and for the heterogeneous problem

$$\mathbf{G} = [\mathbf{D}(\mathbf{A} + \mathbf{B})^{-1} \mathbf{C} - \mathbf{E}], \tag{3.13}$$

$$A_{nm} = -(k^2 + m^2 \pi^2) \int_0^1 R(z) \sin(m\pi z) \sin(n\pi z) dz, \tag{3.14}$$

$$B_{nm} = m\pi \int_0^1 R'(z) \cos(m\pi z) \sin(n\pi z) dz, \tag{3.15}$$

$$C_{nm} = -Rak^2 \int_0^1 \sin((m - 1/2)\pi z) \sin(n\pi z) dz, \tag{3.16}$$

$$D_{nm} = e^{-(m-n-1/2)^2 \pi^2 t} - e^{-(m+n-1/2)^2 \pi^2 t}, \tag{3.17}$$

$$E_{nm} = (k^2 + (n - 1/2)^2 \pi^2) \delta_{nm}. \tag{3.18}$$

For every realization of the resistance field  $R(z)$ , the integrals are computed numerically at the beginning of the calculation. One can also use the linear relation between the vertical velocity and the concentration perturbation to derive the ODEs for  $\widehat{w}_n$ . The amplitude of perturbations in this formulations is then understood to be related to the kinetic energy of the perturbations.

Once the PDEs have been reduced to ODEs of the initial-value type, we are faced with the problem of supplying suitable initial conditions for solving . In principle, one would like to consider the fastest growing perturbations and obtain bounds using these solutions. However, it has been extremely difficult to obtain the fastest growing perturbations due to the time dependence of the base-state. We cannot use the traditional eigenvalue treatments, since the problem is non-autonomous (i.e. the matrix  $\mathbf{G}$  is time dependent). Previous investigators have either solved the initial-value problem with an arbitrarily chosen initial condition (following Foster 1965) or used a quasi-steady-state approximation model and frozen the base-state at some initial instant of time. Clearly, both of these approaches have shortcomings in dealing with

the problem. Recently, the eigenvalue approach has been generalized to deal with problems with extremely non-normal and non-autonomous matrices. This technique is called non-modal stability analysis. Here, we present a brief overview of the idea behind non-modal stability analysis.

Consider the sample vector differential equation

$$\frac{d}{dt}\mathbf{x} = \mathbf{G}(t)\mathbf{x}. \quad (3.19)$$

We now define the ‘propagator’ for this system,  $\mathbf{X}(t, t_0)$ , as

$$\mathbf{x}(t) = \mathbf{X}(t, t_0)\mathbf{x}(t_0); \quad (3.20)$$

i.e. the propagator  $\mathbf{X}$  is a time-dependent matrix which maps the initial condition  $\mathbf{x}(t_0)$  into the solution of the ODE at time  $t$ . Substituting this definition into the ODE, we get

$$\frac{d}{dt}\mathbf{X}(t, t_0) = \mathbf{G}(t)\mathbf{X}(t, t_0), \quad (3.21)$$

which is a matrix-differential equation for the propagator  $\mathbf{X}(t, t_0)$ . However, the advantage with this equation is that the initial condition needed to solve it is known:

$$\mathbf{X}(t_0, t_0) = \mathbf{I}, \quad (3.22)$$

where  $\mathbf{I}$  is the identity matrix. This represents a set of  $N^2$  coupled differential equations for the individual elements of the matrix  $\mathbf{X}(t_n, t_0)$ , where  $N$  is the number of modes used to represent the perturbations, i.e. size of the vector  $\mathbf{x}$ . These equations are integrated in time using a fourth-order Runge–Kutta scheme to obtain the propagator matrix evaluated at discrete times  $t_n = t_0 + n\Delta t$ , where  $\Delta t$  is the time step. At each time step  $t_n$ , the matrix  $\mathbf{X}(t_n, t_0)$  provides a map from every initial condition at  $t = t_0$  to its corresponding final state at  $t = t_n$ . Let us define the amplification achieved by some initial perturbation  $\mathbf{x}_i(t_0)$  as

$$\sigma_i(t_n) = \frac{\|\mathbf{x}_i(t_n)\|}{\|\mathbf{x}_i(t_0)\|}, \quad (3.23)$$

where the final state  $\mathbf{x}_i(t_n)$  can be obtained using the propagator as  $\mathbf{x}_i(t_n) = \mathbf{X}(t_n, t_0)\mathbf{x}_i(t_0)$ . What we are really interested in is the amplification maximized over all possible initial conditions,  $\sigma(t_n) = \max_i \sigma_i(t_n)$ . Let us also simplify by normalizing the initial condition such that  $\|\mathbf{x}(t_0)\| = 1$ . We now have

$$\sigma(t_n) = \max \|\mathbf{X}(t_n, t_0)\mathbf{x}(t_0)\|. \quad (3.24)$$

This is, by definition, the first singular value of the matrix  $\mathbf{X}(t_n, t_0)$  which can be computed using the singular value decomposition (please refer to Golub & Loan 1996). At every time step  $t_n$ , we compute the set of singular values and singular vectors of the matrix  $\mathbf{X}(t_n, t_0)$  and store the first singular value as the growth achieved by the most amplified perturbation. Further, the initial condition  $\mathbf{x}(t_0)$  which leads to this amplification can be obtained as the corresponding right singular vector. Non-modal analysis thus not only provides us with the maximum amplification over all possible initial conditions but also gives us the initial condition which leads to this amplification. For a detailed review of non-modal stability theory, please refer to Farrell & Ioannou (1996a,b) and the recent review by Schmid (2007).

This approach of using singular values to compute the growth of perturbations is exact for any linear system. For the problem of density-dependent convection

in porous media, it can be shown that all perturbations decay in the asymptotic limit  $t \rightarrow \infty$ . This leads to a serious difficulty in defining the onset of convection within the framework of the linearized equations. The physical mechanism of the onset of convection is a nonlinear one – when the perturbations have amplified to a large-enough extent, the nonlinear terms neglected in our analysis become dominant. Previously, we (Rapaka *et al.* 2008) compared the growth of perturbations in homogeneous porous media to those observed in pseudo-spectral simulations and showed that the early fingers manifest themselves when the nonlinear terms begin to dominate. We also showed that the time at which this transition occurs depends on the initial amplitude of the perturbations.

#### 4. Results for anisotropic media

In this section, we present the results obtained for the case of homogeneous porous media with constant anisotropy ratio. In our previous publication ( Rapaka *et al.* 2008) on the isotropic problem, we showed that the onset of instability is marked by the dominance of nonlinear terms neglected in the linear analysis. The extent of magnification required depends on the initial amplitude of perturbations, for which estimates are hard to obtain. For simplicity, in this work we define the ‘critical time of order  $k$ ’,  $t_c^{(k)}$ , as the time at which the most unstable perturbation reaches an amplification of  $10^k$ . For instance, for a given Rayleigh number  $Ra$ ,  $t_c^{(3)}$  is the earliest time at which some perturbation is amplified by a factor of 1000. In a similar sense, the ‘critical Rayleigh number of order  $k$ ’,  $Ra_c^{(k)}$ , is defined to be the smallest Rayleigh number for which some perturbation reaches an amplification by a factor of  $10^k$ .

Using these definition, we first compare our results with those obtained using an initial-value approach. Since the onset of convection occurs far from the bottom boundary, it has been recognized that the critical time and wavenumbers should be insensitive to the boundary conditions applied at the bottom wall. Following the Galerkin procedure presented in Ennis-King *et al.* (2005), we have computed the growth rates of perturbations using both a Dirichlet boundary condition and a Neumann boundary condition at the bottom wall. In figure 1, we compare the critical wavenumbers of order three computed using non-modal analysis with those obtained by Ennis-King *et al.* (2005) using the initial-value approach for both sets of boundary conditions. The Rayleigh numbers in our simulations are different from those used by Ennis-King *et al.* (2005) due to the difference in the definition of critical Rayleigh number. Since we require a minimum amplification of three orders of magnitude, the Rayleigh numbers for our simulations are higher than those used for the initial-value calculation.

We find that the critical wavenumbers computed using non-modal analysis are relatively insensitive to the bottom boundary condition as expected. This reflects the fact that the optimal initial perturbation for both boundary conditions is essentially the same and is captured well by non-modal analysis. An initial condition, such as  $\hat{\theta}_n = 1, \forall n$ , represents a different function for the Dirichlet boundary condition than it does for the Neumann boundary condition, since the eigenfunction basis is different. This is possibly the result for the discrepancy in critical wavenumbers predicted using the initial-value problem.

In their work, Ennis-King *et al.* (2005) also used single-term approximations of the Galerkin expansion to obtain analytical scalings for the dependence of critical Rayleigh number, wavenumber and time for the onset of convection on the anisotropy

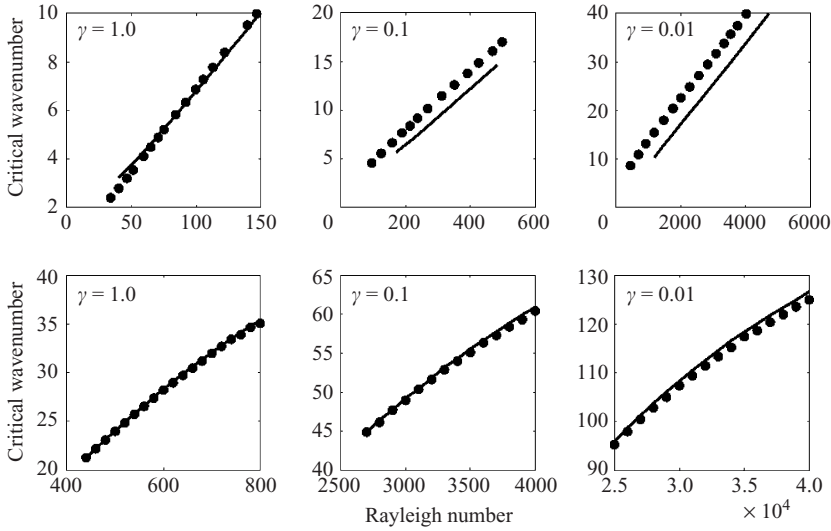


FIGURE 1. Comparison of critical wavenumbers computed using the initial-value approach (above) with those computed using non-modal stability analysis (below). In each case, the solid line corresponds to using a Dirichlet boundary condition at the bottom wall, and the symbols correspond to a Neumann boundary condition. We observe that the results obtained using non-modal analysis are relatively insensitive to the bottom boundary condition, as expected.

ratio  $\gamma$  :

$$Ra_c(\gamma)/Ra_c(1) \sim \frac{(1 + \sqrt{\gamma})^2}{4\gamma}, \tag{4.1}$$

$$t_c(\gamma)/t_c(1) \sim \frac{(1 + \sqrt{\gamma})^4}{16\gamma^2}, \tag{4.2}$$

$$s_c(\gamma)/s_c(1) \sim \frac{(1 + \sqrt{\gamma})^2}{4\gamma^{3/4}}. \tag{4.3}$$

In figure 2 we show the comparison between the scalings proposed by Ennis-King *et al.* (2005) and those obtained using the non-modal stability calculation for critical values of order zero (solid line) and order three. It can be seen that the values computed from non-modal theory correspond closely with those predicted by Ennis-King *et al.* (2005).

The critical values of the Rayleigh number presented so far are values computed over large time scales. For engineering purposes, one is interesting in knowing the medium properties (permeability, porosity, etc.) needed to ensure that the perturbations amplify a certain amount in a specified amount of time. We have used non-modal stability analysis to compute critical Rayleigh numbers conditioned on the maximum time at which the perturbations amplify by a factor of  $10^3$ . We have computed the smallest Rayleigh number needed to achieve a perturbation amplification of a factor of  $10^3$  for  $t < 0.01$ ,  $t < 0.1$  and  $t < 1.0$ . In figure 3, we show the phase diagram of the different critical Rayleigh numbers as a function of the anisotropy ratio  $\gamma$ . The critical Rayleigh number in the long-time limit for the isotropic problem ( $\gamma = 1.0$ ) is seen to be close to the well-known value of  $4\pi^2$  obtained by previous investigators. It can be seen that requiring the critical time to be less that

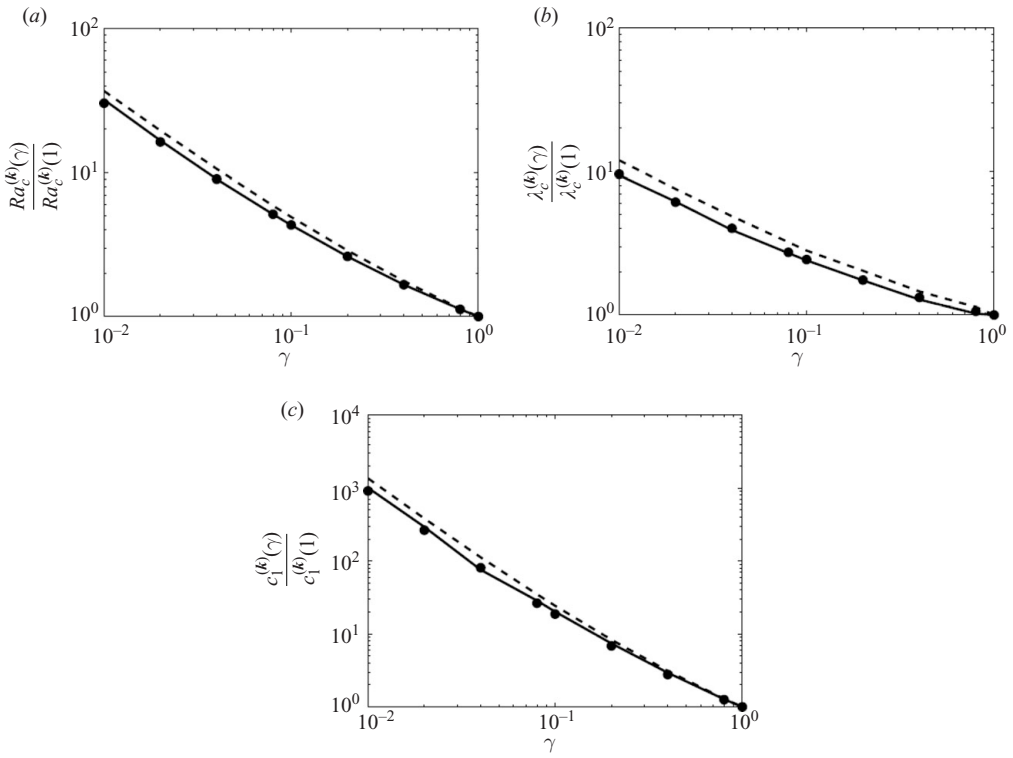


FIGURE 2. Dependence of the critical (a) Rayleigh numbers  $Ra_c^{(k)}$ , (b) wavelengths  $\lambda_c^{(k)} = 2\pi Ra_c^{(k)}/s_c^{(k)}$  and (c) time scales  $c_1^{(k)}(\gamma) = Ra_c^{(k)2} t_c^{(k)}$  on the anisotropy ratio  $\gamma$ : symbols, analytical scaling predicted by Ennis-King *et al.* (2005); solid line,  $k=0$ ; dashed line,  $k=3$ .

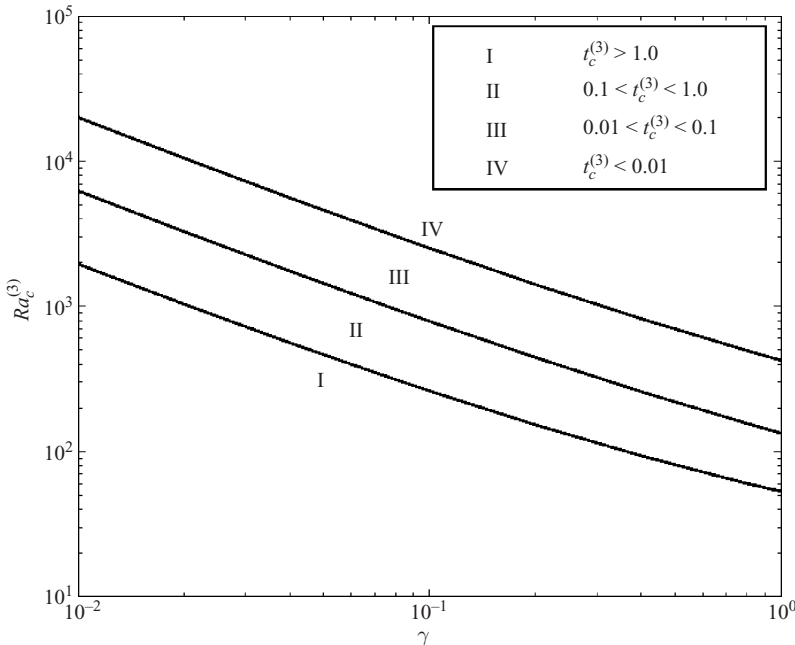


FIGURE 3. Phase diagram of the critical Rayleigh numbers  $Ra_c^{(3)}$  as a function of the anisotropy ratio  $\gamma$  for different values of  $t_{max}$ . For a given Rayleigh number and anisotropy ratio, this plot can be used to determine the time for the perturbations to amplify by a factor of 1000.

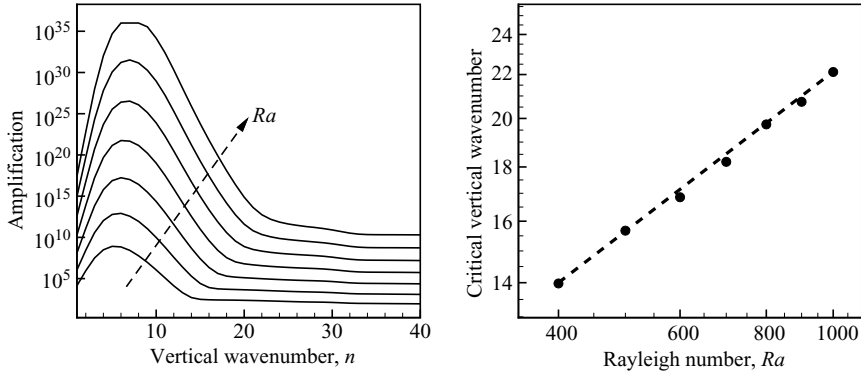


FIGURE 4. Maximum amplification achieved by any perturbation for sinusoidal permeability fields of the form  $\log R(z) = -\sin(n\pi z)$ . It is observed that the permeability variation has a strong effect for low wavenumbers with a cutoff wavenumber after which fluctuations are not important. (a) Maximum amplification versus vertical wavenumber for  $Ra$  varying between 400 and 1000 in steps of 100. (b) The dependence of the cutoff wavenumber on the Rayleigh number  $Ra$ : symbols, non-modal theory; dashed line,  $n \sim Ra^{1/2}$ .

0.01 increases the minimum Rayleigh number by a factor of 10. Given the properties of a particular site, this plot can also be used to estimate the time needed for the onset of convection.

## 5. Results for heterogeneous systems

In this section, we will present results relevant to heterogeneous porous media with a dominant layering structure. To this effect, we have used non-modal stability theory to compute the growth of perturbations for simple permeability fields of the form  $\log R(z) = \delta \sin(n\pi z)$ , where  $n$  is the wavenumber associated with permeability variation in the vertical direction.

### 5.1. Effect of characteristic-length scale

We used permeability fields of the form  $\log R(z) = \delta \sin(n\pi z)$  for  $n$  taking all integer values between 1 and 40. We used  $\delta = -1$  in all the simulations, resulting in decreasing resistance to flow at the top of the domain, i.e. for  $z \in [0, 1/2n]$ . We used the first 32 modes in the Galerkin expansion of concentration fluctuation and computed the amplification of perturbations for  $0 \leq t \leq 0.01$ . The horizontal wavenumber was varied between  $k = \pi$  and  $k = 50\pi$ .

In figure 4, we show the maximum amplification achieved by the perturbations as a function of the wavenumber  $n$  corresponding to variation in the vertical direction. It is seen that there are two distinct regimes in this plot. For sufficiently low values of  $n$ , the variations in permeability have a very strong influence on the growth of perturbations, whereas at higher values of  $n$  the system seems to be relatively unaffected by the wavenumber. The wavenumber at which this behaviour changes is associated with the diffusive length scale  $l = \sqrt{Dt}$ . Permeability variations below this length scale have only a small influence on the growth of perturbations, whereas variations in permeability at larger length scales have a very strong influence. Since the only non-dimensional parameter for this problem is the Rayleigh number which depends on the diffusion coefficient as  $D^{-1}$ , we expect the transition wavenumber to scale as  $n \sim Ra^{1/2}$ .

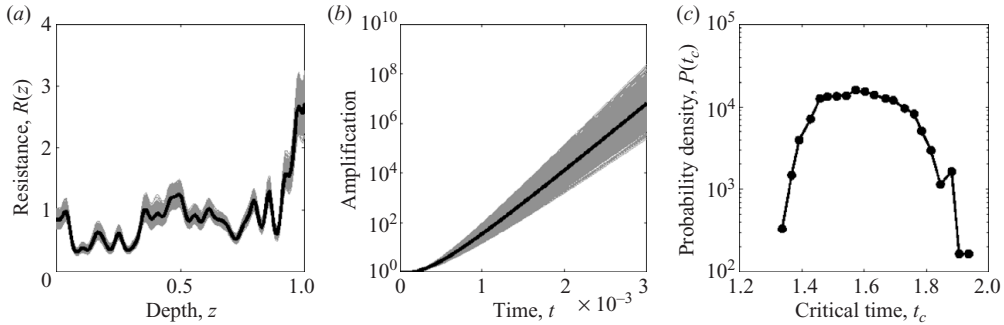


FIGURE 5. (a) Sample resistance fields generated for uncertainty quantification. The bold line is the base resistance field. (b) Growth of perturbations for the different realizations. The bold line corresponds to the base field. (c) The probability density of critical times observed. The mean critical time was  $1.6 \times 10^{-3}$  with a standard deviation of  $1.2 \times 10^{-4}$  when  $Ra = 900$ .

Figure 4 shows that variations of permeability at low wavenumbers has a very strong influence on the dynamics of perturbations. Since the permeability data can never be obtained exactly, this simulation underscores the importance of uncertainty quantification for heterogeneous media. It is possible to undertake such a task using a Monte Carlo approach. We generated a set of 1000 permeability fields, obtained by adding perturbations to a base field, and calculated the growth of perturbations for this set of realizations. In figure 5(a), the different realizations are shown along with the base resistance field (bold line). The amplifications computed for the different realizations are shown in figure 5(b). The simulations were performed using a Rayleigh number of  $Ra = 900$ . The permeability field has a relatively mild heterogeneity, with a variation less than one order of magnitude. We can now use the times at which each system attains three orders of magnitude amplification, to generate the probability distribution function of the critical time for this system. In figure 5(c), we show the probability density function for the critical times. The mean critical time was found to be  $1.6 \times 10^{-3}$  with a standard deviation of  $1.2 \times 10^{-4}$ .

### 5.2. Comparison with simulations

For engineering purposes, we are interested in real porous media which are heterogeneous in all directions. For the purposes of this paper, our interest is in those fields in which the typical variation of permeability in the vertical direction is much larger than that in the horizontal directions. To make this definition more formal, we define a parameter  $\alpha$  as the ratio of the norms of permeability gradients in the horizontal and vertical directions:

$$\alpha = \frac{\|\partial_x K\|}{\|\partial_z K\|}.$$

The case  $\alpha = 0$  corresponds to a strictly layered porous medium (variation only in the vertical direction), where the limit  $\alpha = 1$  corresponds to an isotropic porous medium. The growth of perturbations calculated using non-modal analysis is expected to be useful whenever  $\alpha \ll 1$ .

We will first describe the technique used for generating the heterogeneous permeability fields. The permeability fields are generated by adding an isotropic random fluctuation field to a strictly layered permeability field:

$$\log K(x, z) = \log K_0(z) + \epsilon \zeta(x, z). \quad (5.1)$$

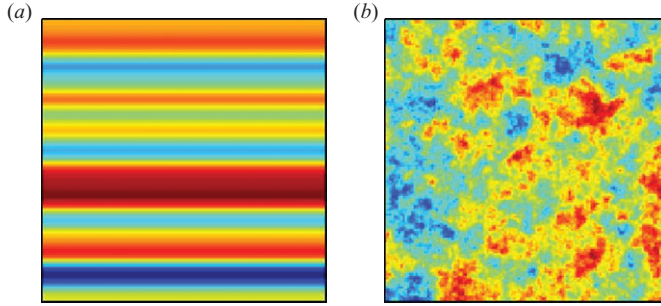


FIGURE 6. (a) The one-dimensional base permeability field with no variations in the horizontal direction. (b) An isotropic permeability fluctuation, generated using the turning-bands algorithm.

We have also ensured that the horizontal mean along any slice of  $\zeta(x, z)$  vanishes, so that the horizontally averaged  $\log K(x, z)$  is the same as  $\log K_0$ :

$$\int \zeta(x, z) dx = 0, \forall z. \quad (5.2)$$

The isotropic fields are generated using the turning-bands method (Mantoglou & Wilson 1982) and modified to ensure zero mean along each horizontal slice. The turning-bands algorithm replaces the task of generating a high-dimensional random field with a given covariance function with the generation of a finite number of one-dimensional random functions along lines passing through an arbitrarily chosen origin (typically taken to be at the centre of the domain, for convenience). The value of the random field at each grid point is then obtained using the average of projections from each line. Owing to the reduction in dimensionality of the problem, random fields can be generated extremely rapidly by using this approach.

By varying  $\epsilon$  in (5.1), it is possible to control the value of  $\alpha$ . On the other hand, given a value of  $\alpha$ , we can compute  $\epsilon$  by using any standard root-finding technique. As an example, we consider the one-dimensional log-permeability field and the isotropic fluctuation shown in figure 6. By choosing different values of  $\epsilon$ , it is possible to obtain heterogeneous structures characterized by different values of  $\alpha$ . We used this technique to generate permeability fields with  $\alpha$  varying from 0.1 to 0.9 in increments of 0.1. These structures are shown in figure 7.

To compare the predictions of stability theory with two-dimensional heterogeneous media, we developed a staggered-grid finite-volume solver for the governing equations (Ferziger & Peric 2001). The pressure and concentration of dissolved  $\text{CO}_2$  are stored at the centre of the grid cell, whereas the fluid velocities are defined on the corresponding edges. The equations are integrated in time using a second-order Adams–Bashforth technique, and a Runge–Kutta time-stepping algorithm is used for the first time step. The finite-volume solver was tested by comparing the results obtained for a homogeneous system with those obtained using a pseudo-spectral solver.

The finite-volume simulations are initialized using the analytical base-state at  $t = 10^{-4}$ . The initial concentration field is perturbed by adding a Gaussian, spatially uncorrelated noise field. In our previous publication (Rapaka *et al.* 2008), we showed that when the simulations are initialized using the most amplified initial perturbation, the growth of perturbations matches extremely well with those predicted from theory. When the initial perturbation is taken to be random noise, there is significant decay

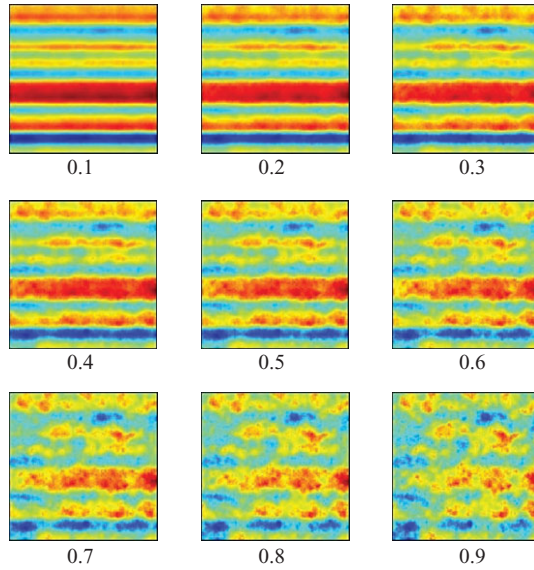


FIGURE 7. Sample permeability fields generated using a linear combination of the fields shown in figure 6, labelled by their value of  $\alpha$ . The proportion of isotropic fluctuation added is chosen to yield the required value of  $\alpha$ .

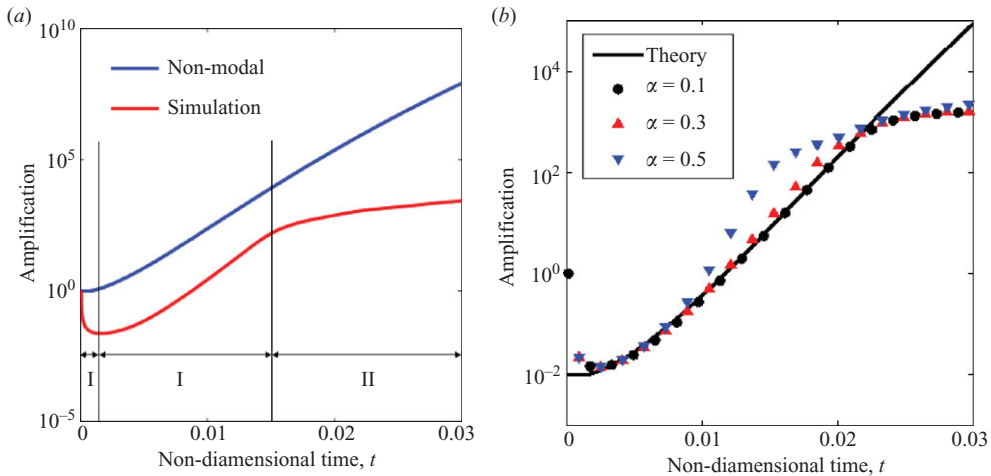


FIGURE 8. (a) Comparison of the amplification predicted by non-modal theory (blue line) to that obtained in a finite-volume simulation (red line) with  $\epsilon = 10^{-3}$ . We observe three distinct regions in the growth from numerical simulations: (I) an initial transient period of rapid relaxation of sub-optimal modes, (II) growth of perturbations which agrees well with that predicted by the theory and (III) nonlinear growth of the fingers. (b) Comparison of the growth rates obtained from simulations with different values of  $\alpha$ . The Rayleigh number is  $Ra = 400$ , and log permeability has a standard deviation of 1.0. The curve corresponding to non-modal theory has been scaled down by a factor of 100 for ease of comparison.

of perturbations initially due to the rapid relaxation of the sub-optimal modes. Very soon, the perturbation resolves itself to the dominant mode after which the growth of perturbations is expected to match the theoretical prediction. In figure 8(a), we compare the growth of perturbations predicted from theory with those obtained from

a finite-volume simulation. As expected, we observe an initial decay period in which the energy in the perturbations drops sharply and the perturbation resolves itself to the dominant mode. Beyond this, the growth of the perturbation agrees extremely well with that predicted by the theory. At some point during this growth process, the perturbations become strong enough that the nonlinear terms neglected in the stability theory become dominant. After this point of time, the growth of perturbations in the simulation begins to deviate from the theoretical prediction.

To study the influence of  $\alpha$ , we generated many realizations such as those shown in figure 7. For each realization, the finite-volume solver was used to compute the growth of perturbations in the heterogeneous system. In figure 8(b), we present the results obtained for permeability fields (same as those shown in figure 7) with different values of  $\alpha$ . For these simulations, the Rayleigh number is  $Ra = 400$ , and the permeability variation has a standard deviation of 1.0. The predictions obtained from non-modal theory agree extremely well with the simulations for low values of  $\alpha$ . When  $\alpha = 0.1$ , the agreement between theory and simulations is almost exact. At  $\alpha = 0.3$ , the simulations begin to show slightly higher growth than that predicted by theory. Over tests done with multiple realizations, we observed that the results from non-modal theory remain useful as long as  $\alpha \leq 0.25$ . For  $\alpha > 0.25$ , the isotropic component of permeability creates ‘bridges’ between high-permeability layers which were originally separated by a low-permeability barrier. This results in a faster growth of perturbations in the simulations compared to those predicted by the theory.

## 6. Discussion

The main contribution of this paper is a theoretical model for predicting growth of perturbations in anisotropic and heterogeneous porous media. From an engineering perspective, most field measurements are obtained using vertical wells and give us detailed information about the variation of permeability and porosity in the vertical direction. When combined with multiple measurements at different locations, the data can give a reasonable estimate of the three-dimensional structure of the reservoir.

In this work, we have presented a theoretical model that can rapidly produce the growth of perturbations in layered formations. We have shown that this model remains useful as long as the gradients of permeability in the horizontal direction are much smaller than those in the vertical direction. Owing to the speed of calculations, this method can also be used as a tool to perform uncertainty analysis using a Monte Carlo approach. For a given variation of permeability in the vertical direction, we can generate a large array of cases which account for deviations from the available data. By using the growth of perturbations over this sample space, we can obtain the probability distribution functions of the critical time and length scales. Nield and coworkers (see Nield & Simmons 2007 and Nield, Kuznetsov & Simmons 2009) have addressed the issue of an effective Rayleigh number for the onset of Horton–Rogers–Lapwood convection in heterogeneous porous media. To our knowledge, this is the first publication which addresses this issue for the problem of transient convection.

The authors would like to thank Professor Gregory Eyink and Professor Andrea Prosperetti for valuable discussions. Saikiran Rapaka would like to thank Professor Robert McKibbin and Professor Peder Tyvand for comments on the relation between anisotropy and horizontal layering. The simulations were performed on a computational cluster supported by the NSF under grant nos CBET-0320907 and AST-0428325.

## REFERENCES

- BECK, J. L. 1972 Convection in a box of porous material saturated with fluid. *Phys. Fluids* **15**, 1377–1383.
- BRAESTER, C. & VADASZ, P. 1993 The effect of a weak heterogeneity of a porous medium on natural convection. *J. Fluid Mech.* **254**, 345–362.
- CASTINEL, G. & COMBARNOUS, M. 1977 Natural convection in an anisotropic porous medium. *Intl Chem. Engng* **17**, 605–613.
- CHENG, P. 1978 Heat transfer in geothermal systems. *Adv. Heat Transfer* **14**, 1–105.
- CURRIE, I. G. 1967 The effect of heating rate on the stability of stationary fluids. *J. Fluid Mech.* **29**, 337–347.
- ELDER, J. W. 1967 Transient convection in a porous medium. *J. Fluid Mech.* **27**, 609–623.
- ENNIS-KING, J., PRESTON, I. & PATERSON, L. 2005 Onset of convection in anisotropic porous media subject to a rapid change in boundary conditions. *Phys. Fluids* **17** (8), 084107.
- EPHERRE, J. F. 1977 Criterion for the appearance of natural convection in an anisotropic porous layer. *Intl Chem. Engng* **17**, 615–616.
- FARRELL, B. F. & IOANNOU, P. J. 1996a Generalized stability theory. Part I. Autonomous operators. *J. Atmos. Sci.* **53** (14), 2025.
- FARRELL, B. F. & IOANNOU, P. J. 1996b Generalized stability theory. Part II. Nonautonomous operators. *J. Atmos. Sci.* **53** (14), 2041.
- FERZIGER, J. H. & PERIC, M. 2001 *Computational Methods for Fluid Dynamics*. Springer.
- FOSTER, T. D. 1965 Stability of a homogeneous fluid cooled uniformly from above. *Phys. Fluids* **8** (7), 1249–1257.
- GARCIA, J. E. 2001 Density of aqueous solutions of CO<sub>2</sub>. *Tech Rep.* LBNL-49023. Lawrence Berkeley National Laboratory.
- GOLUB, G. H. & LOAN, C. F. VAN 1996 *Matrix Computations*. Johns Hopkins University Press.
- HASSANZADEH, H., POOLADI-DARVISH, M. & KEITH, D. W. 2006 Stability of a fluid in a horizontal saturated porous layer: effect of nonlinear concentration profile, initial, and boundary conditions. *Transp. Porous Med.* **65** (2), 193–211.
- HITCHON, B. 1996 *Aquifer Disposal of Carbon Dioxide: Hydrodynamic and Mineral Trapping*. Alberta Research Council.
- HORTON, C. W. & ROGERS, F. T., JR 1945 Convection currents in a porous media. *J. Appl. Phys.* **16**, 367–370.
- INTERGOVERNMENTAL PANEL ON CLIMATE CHANGE (IPCC) 2005 *IPCC Special Report on Carbon Dioxide Capture and Storage. Prepared by Working Group III of the Intergovernmental Panel on Climate Change (B. Metz, O. Davidson, H. C. de Coninck, M. Loos and L. A. Meyer)*. Cambridge University Press.
- JHAVERI, B. S. & HOMS, G. M. 1982 The onset of convection in fluid layers heated rapidly in a time-dependent manner. *J. Fluid Mech.* **114**, 251–260.
- JOSEPH, D. D. 1976 *Stability of Fluid Motions I*, Tracts in Natural Philosophy, vol. 27. Springer.
- KIM, M. C. & CHOI, C. K. 2007 Relaxed energy stability analysis on the onset of buoyancy-driven instability in the horizontal porous layer. *Phys. Fluids* **19**, 088103.
- KVERNOLD, O. & TYVAND, P. A. 1979 Nonlinear thermal convection in an anisotropic porous media. *J. Fluid Mech.* **90**, 609–624.
- LAPWOOD, E. R. 1948 Convection of a fluid in a porous medium. *Proc. Camb. Phil. Soc.* **44**, 508–521.
- LEONG, J. C. & LAI, F. C. 2001 Effective permeability of a layered porous cavity. *ASME J. Heat Transfer* **123**, 512–519.
- LICK, W. 1965 The instability of a fluid layer with time-dependent heating profile. *J. Fluid Mech.* **21**, 565.
- MANTOGLOU, A. & WILSON, J. L. 1982 The turning bands method for simulation of random fields using line generation by a spectral method. *Water Resour. Res.* **18**, 1379–1394.
- MCKIBBIN, R. & O'SULLIVAN, M. J. 1980 Onset of convection in a layered porous medium heated from below. *J. Fluid Mech.* **96** (2), 375–393.
- MCKIBBIN, R. & TYVAND, P. A. 1982 Anisotropic modelling of thermal convection in multilayered porous media. *J. Fluid Mech.* **118**, 315–339.
- NIELD, D. A. 1994 Estimation of an effective Rayleigh number for convection in a vertically inhomogeneous porous medium or clear fluid. *Intl J. Heat Fluid Flow* **15**, 337–340.

- NIELD, D. A. 1997 Notes on convection in a porous medium: (i) an effective Rayleigh number for an anisotropic layer, (ii) the Malkus hypothesis and wavenumber selection. *Transp. Porous Med.* **27**, 135–142.
- NIELD, D. A. & BEJAN, A. 2006 *Convection in Porous Media*, 3rd edn. Springer.
- NIELD, D. A., KUZNETSOV, A. V. & SIMMONS, C. T. 2009 The effect of strong heterogeneity on the onset of convection in a porous medium: non-periodic global variation. *Transp. Porous Med.* **77**, 169–186.
- NIELD, D. A. & SIMMONS, C. T. 2007 A discussion on the effect of heterogeneity on the onset of convection in a porous medium. *Transp. Porous Med.* **68**, 413–421.
- NILSEN, T. & STORESLETTEN, L. 1990 An analytical study on natural convection in isotropic and anisotropic porous channels. *J. Heat Transfer* **112**, 396–401.
- PRASAD, A. & SIMMONS, C. T. 2003 Unstable density-driven flow in heterogeneous porous media: a stochastic study of the Elder (1967*b*) ‘short heater’ problem. *Water Resour. Res.* **39** (1), 1007.
- RAPAKA, S., CHEN, S., PAWAR, R. J., STAUFFER, P. H. & ZHANG, D. 2008 Nonmodal growth of perturbations in density-driven convection in porous media. *J. Fluid Mech.* **609**, 285–303.
- RIAZ, A., HESSE, M., TCHELEPI, H. A. & ORR JR., F. M. 2006 Onset of convection in a gravitationally unstable diffusive boundary layer in porous media. *J. Fluid Mech.* **548**, 87–111.
- SCHMID, P. J. 2007 Nonmodal stability theory. *Annu. Rev. Fluid Mech.* **39**, 129–162.
- SIMMONS, C. T., FENSTEMAKER, T. R. & SHARP, J. M. 2001 Variable-density groundwater flow and solute transport in heterogeneous porous media: approaches, resolutions and future challenges. *J. Contam. Hydrol.* **52**, 245–275.
- STAUFFER, P. H. 2006 Flux flummoxed: a proposal for consistent usage. *Ground Water* **44** (2), 125–128.
- STRAUGHAN, B. 2004 *The Energy Method, Stability and Nonlinear Convection*. Springer.
- TAN, C. T. & HOMS, G. M. 1986 Stability of miscible displacements in porous media: rectilinear flow. *Phys. Fluids* **29** (11), 3549–3556.
- TREFETHEN, L. N. & EMBREE, M. 2005 *Spectra and Pseudospectra: The Behaviour of Nonnormal Matrices and Operators*. Princeton University Press.
- TYVAND, P. A. & STORESLETTEN, L. 1991 Onset of convection in an anisotropic porous medium with oblique principal axes. *J. Fluid Mech.* **226**, 371–382.
- WOODING, R. A. 1978 Large-scale geothermal field parameters and convection theory. *NZ J. Sci.* **27**, 219–228.
- XU, X., CHEN, S. & ZHANG, D. 2006 Convective stability analysis of the long-term storage of carbon dioxide in deep saline aquifers. *Adv. Water Resour.* **29**, 397–407.